Bulletins of Research Institute of Marine Science and Technology
Korea Maritime University, Vol. 4, pp. 103 - 113, December 1995.

Marine Structures 8 (1995) 543–553

0951-8339/95/$9.50

Tensioned Buoyant Platform Tether Response to Short Duration Tension Loss

M. H. Patel[a] & H. I. Park[b]

[a]Department of Mechanical Engineering, University College London, Torrington Place, London, UK, WC1E 7JE

[b]Department of Ocean Engineering, Korea Maritime University, Youngdo-ku, Pusan, South Korea

(Received 8 October 1993)

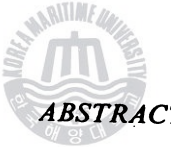

ABSTRACT

In conventional design practice, the tethers of tensioned buoyant platforms are operated at a sufficiently high pre-tension so as not to go slack in combinations of extreme environmental conditions — such as a 100 year return period sea state combined with low tide and high platform variable load. This high pre-tension imposes a significant payload and structural weight penalty and is a motivation for investigation of TBP tether performance at low tensions.

TPB tethers operated at lower mean tension would be prone to short duration tension losses in extreme design case conditions. This is likely to remain true despite the possibility of lower anchor connectors being able to alleviate this tension loss by dropping down from their restraints. This paper presents the results of an investigation into tether behaviour under transient tension loss by solving the governing equation of lateral tether motions both analytically and numerically. The resultant amplification functions and preferred modes of tether deformation are used for an example tether to obtain criteria for allowable tension loss and duration time to first attainment of maximum stress in the tether material.

It is shown that tension loss lasting a few seconds during the passage of an extreme wave can be designed to be acceptable for typical tether structures.

Key words: tensioned buoyant platform, tension loss.

1 INTRODUCTION

The technology of tensioned buoyant platforms (TBPs) is reaching a phase where cost reduction by refinement of platform and tether designs is growing in priority. TBPs have conventionally been designed with really quite substantial margins of tether pre-tension so as not to lose all tensions under combined occurrences of extreme waves, low tide levels and high platform variable weight. These high margins lead to penalties in structural weight and payload growth which could be alleviated by considering the design and operation of TBPs at lower tether tensions.

Previous work on TBPs[1] has shown that as pre-tension is reduced, time-varying axial forces play an important role in increasing lateral motions of the tethers but that this lateral motion is still limited by quadratic damping in water. In these cases of reduced tension, acceptable platform and tether motions are achievable in normal and moderately severe operating conditions. However, during combined occurrences of extreme wave, tide and variable weight, individual tether tensions will reduce to zero and become compressive for part of a wave cycle. This transient tension loss can also be defined as a dynamic pulse buckling phenomenon — the application of an axial compressive force larger than the static Euler buckling value for a short period of time.

In dynamic pulse buckling, it is known that a slender column can survive (with acceptable stress levels), a sudden compressive axial load much greater than the static Euler load as long as the load duration is short enough. Pulse buckling has been extensively studied in other branches of engineering — for example, in the design of aircraft landing struts, ballistic missiles and shock- or blast-resistant structures. An early researcher in this field investigated time deflection relationships when an axial force was very rapidly applied to a nearly straight bar.[2] Following this work, the dynamic pulse buckling problem for slender bar-type structures was extensively studied by many researchers.[3-6] Lindberg and Florence, in their book of 1987,[7] presented an integrated treatment of dynamic pulse buckling including much of the research carried out in the last two decades. However, all of this work has been carried out for structures in air with pure axial forcing and no lateral added mass or quadratic damping effects.

This paper presents an extension of the theory of pulse buckling for the tethers of TBPs. This is done by developing and analytically solving the governing equation of tether lateral motion for pulse buckling behaviour. The solution yields an amplification function and modes of deformation which are used to obtain an envelope of compressive axial load against duration to maintain acceptable stress levels in a typical tether.

2 GOVERNING EQUATION AND SOLUTION

The adopted idealisation is shown in Fig. 1 and the corresponding governing equation of lateral motion is given as

$$(m_s + m_a)\frac{\partial^2 y}{\partial t^2} + EI\frac{\partial^4 y}{\partial x^4} + P_c\frac{\partial^2 (y + y_i)}{\partial x^2} + B_v\left|\frac{\partial y}{\partial t}\right|\frac{\partial y}{\partial t} = 0 \qquad (1)$$

where EI is flexural rigidity, P_c is tension loss, m_s is physical mass per unit length, m_a is added mass per unit length, B_v is damping coefficient, and y_i is initial deflection of tendon.

It is noted that dynamic pulse buckling involves very high modes so the

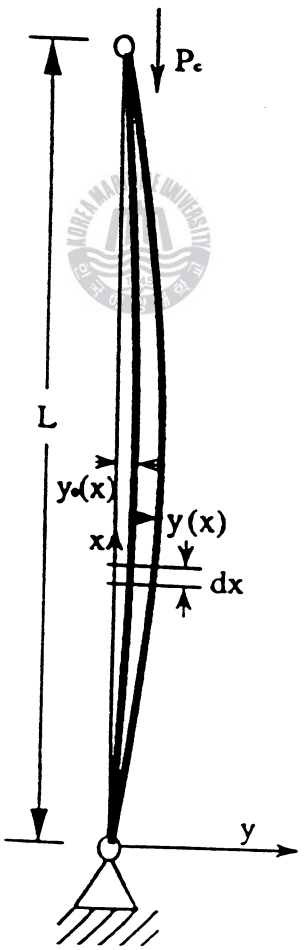

Fig. 1. Pulse load condition of tether.

bending stiffness force is important even for the long cylinder case. The following parameters are introduced for convenience:

$$k^2 = \frac{P_c}{EI} \quad r^2 = \frac{I}{A_s} \quad c^2 = \frac{A_s E}{m_s} \quad e^2 = 1 + \frac{m_a}{m_s} \tag{2}$$

where E is the modulus of elasticity and I is the second moment of area of the structure with cross-sectional area, A_s. Equation (1) becomes

$$\frac{e^2}{r^2 c^2}\frac{\partial^2 y}{\partial t^2} + \frac{\partial^4 y}{\partial x^4} + k^2\frac{\partial^2 y}{\partial x^2} + \frac{B_v}{EI}\left|\frac{\partial y}{\partial t}\right|\frac{\partial y}{\partial t} = -k^2\frac{\partial^2 y_i}{\partial x^2} \tag{3}$$

In the case where high modes become dominant, it is useful to express eqn (3) in a non-dimensional form. Instead of the actual structure length, ξ is adopted as a characteristic length because the wavelengths of interest in pulse buckling are very short in comparison to the total length of a typical TBP tether. Thus, the actual length of the tether has a negligible influence on the response and for practical purposes even the shortest feasible TBP tether length would still fall within the range of being very much larger than pulse buckling wavelengths. Similarly, it is usual to normalise lateral deflections with respect to the radius of gyration, r of the structure cross-section. The following non-dimensional variables are introduced:

$$w = y/r \quad \xi = kx \quad \tau = (k^2 rct)/e \quad \beta = (B_v r)/(m_s + m_a) \tag{4}$$

where $B = 0{\cdot}5\,\rho_w C_d d_0$ and $r = \sqrt{I/A_s}$ with $\rho_w C_d$ and d_0 denoting sea water density, drag coefficient and tether outer diameter, respectively.

Equation (3) can be then expressed in a non-dimensional form as

$$\frac{\partial^2 w}{\partial \tau^2} + \frac{\partial^4 w}{\partial \xi^2} + \frac{\partial^2 w}{\partial \xi^2} + \beta\left|\frac{\partial w}{\partial \tau}\right|\frac{\partial w}{\partial \tau} = -\frac{\partial^2 w_i}{\partial \xi^2} \tag{5}$$

The boundary conditions are

$$w = \frac{\partial^2 w}{\partial \xi^2} = 0 \quad \text{at } \xi = 0 \quad \text{and} \quad \xi = l(= kL)$$

For the above boundary conditions, the solution of eqn (5) can be put in the following form:

$$w(\xi, \tau) = \sum_{n=1}^{\infty} g_n(\tau)\sin\eta\xi \tag{6}$$

$$w_i(\xi) = \sum_{n=1}^{\infty} a_n(\tau)\sin\eta\xi \tag{7}$$

where an axial wave number η is introduced by

$$\eta = n\pi/l \tag{8}$$

and g_n, a_n are Fourier coefficients for the response deflection and initial deflection, respectively.

Substituting eqns (6) and (7) into eqn (5) gives

$$\frac{d^2 g_n}{d\tau^2} + \varepsilon\left|\frac{dg_n}{d\tau}\right|\frac{dg_n}{d\tau} + \eta^2(1-\eta^2)g_n = \eta^2 a_n \tag{9}$$

where $|\sin\eta\xi|\sin\eta\xi = (8/3)\pi\sin\eta\xi$ is used and thus

$$\varepsilon = 8\beta/3\pi \tag{10}$$

The solution of eqn (9) becomes hyperbolic for $\eta < 1$ and trigonometric for $\eta > 1$. The trigonometric form gives stable motion, that is, the compressive axial force is less than the Euler buckling load. Thus, only the hyperbolic form is considered here. For such a condition, eqn (9) becomes

$$\frac{d^2 g_n}{d\tau^2} + \varepsilon\left|\frac{dg_n}{d\tau}\right|\frac{dg_n}{d\tau} - \eta^2(1-\eta^2)g_n = \eta^2 a_n \tag{11}$$

The non-linear damping term makes it difficult to obtain an exact closed-form solution for eqn (11). An approximate closed-form solution is obtained in the following form:[1]

$$\text{for } 0 < \tau < \frac{1}{\sqrt{\eta^2(1-\eta^2)}}\, l_n \frac{2(1-\eta^2)}{\varepsilon a_n}$$

$$g_n(\eta,\tau) = \frac{a_n}{(1-\eta^2-2\varepsilon a_n)}\left\{\cosh\left[\sqrt{1-\frac{2\varepsilon a_n}{1-\eta^2}}\times\sqrt{\eta^2(1-\eta^2)}\tau\right] - 1\right\} \tag{12}$$

where l_n is the wavelength corresponding to response amplitude g_n;

$$\text{for } \tau > \frac{1}{\sqrt{\eta^2(1-\eta^2)}}\, l_n \frac{2(1-\eta^2)}{\varepsilon a_n}$$

$$g_n(\eta,\tau) = \frac{1}{2\varepsilon}\frac{a_n}{(1-\eta^2)} + \frac{1}{4\varepsilon}\left\{\sqrt{\eta^2(1-\eta^2)}\tau - l_n\frac{2(1-\eta^2)}{\varepsilon a_n} + 2\sqrt{0{\cdot}5 + \frac{\varepsilon a_n}{(1-\eta^2)}}\right\}^2 \tag{13}$$

Equation (11) can also be solved numerically by using the fourth-order Runge–Kutta method.

When hydrodynamic damping is not considered, i.e. $\varepsilon = 0$, the solution can be given in the following form by putting $\varepsilon = 0$ in eqn (12):

$$g_n(\eta, \tau) = \frac{a_n}{(1-\eta^2)}(\cosh \eta \sqrt{1-\eta^2}\,\tau - 1) \tag{14}$$

3 PREFERRED MODE OF BUCKLING

The ratio between the Fourier coefficient, a_n, of the initial deflection and the coefficient $g_n(\tau)$ of the response deflection is called the amplification function and is expressed as follows:

$$G_n(\tau) = \frac{g_n(\tau)}{a_n} = \frac{1}{1-\eta^2}[\cosh(\eta\sqrt{1-\eta^2}\,\tau) - 1] \tag{15}$$

The preferred mode, i.e. the most amplified mode, can be obtained by differentiating the amplification function with regard to wave number and setting the result to zero. It should be said that this is done for $\varepsilon = 0$, that is, without viscous damping. It is assumed that hydrodynamic damping does not affect the preferred mode of buckling since the preferred mode is initiated before the hydrodynamic damping forces come into effect. Using this argument, the preferred mode of buckling can be obtained by finding η which satisfies the following condition:

$$\frac{dG}{d(\eta^2)} = 0 \tag{16}$$

Then the resulting preferred mode is taken as

$$\eta_{cr} = 1/\sqrt{2} \tag{17}$$

or

$$n_{cr} = \frac{1}{\sqrt{2}}\sqrt{\frac{\tau}{\tau - 2}}$$

for a better estimate. This solution is obtained from eqn (16) and is also a turning point of eqn (15). The corresponding wavelength is found from

$$\eta_p \xi_p = 2\pi \quad \text{or} \quad \xi_p \equiv 2\pi\sqrt{2} \tag{18}$$

by replacing η_p with η_{cr}.

The corresponding wave length in dimensional units is obtained from eqn (4) as

$$x_p = 8{\cdot}88/k \tag{19}$$

4 ESTIMATES OF CRITICAL TIME AND APPLIED FORCE

Imperfections (initial deflections) can be divided into two types: one type having amplitudes proportional to the radius of gyration of the structure cross-sectional area, and the other having amplitudes proportional to the wave length of the buckling. It was shown by Lindberg and Florence[7] that the critical times τ_{cr} for buckling do not depend strongly upon which type is assumed. Here, imperfections (initial deflections) having amplitudes proportional to the radius of gyration of the structure cross-section are used.

The initial imperfection is assumed as

$$A_p = \gamma r \tag{20}$$

In a non-dimensional form

$$a_p = \gamma = 0{\cdot}2r/d_0 \tag{21}$$

The criteria for buckling of the structure is taken to be when the bending stress (σ_b) plus the compressive axial stress (σ_c) due to P_c reaches 67% of the yield stress (σ_y), i.e.

$$\sigma_b + \sigma_c = 0{\cdot}67\sigma_y \tag{22}$$

The bending stress for the column-type structure is

$$\sigma_b = \frac{E d_0 k^2 r}{2} \frac{\partial^2 w}{\partial \xi^2} \tag{23}$$

and the radius of gyration of the cylindrical structure cross-section is

$$r = \sqrt{\frac{d_0^2 - d_i^2}{16}} \tag{24}$$

where d_0 and d_i are the outer and inner diameters of the tether, respectively.

Thus, substituting eqns (24) and (2) into eqn (22) yields

$$\sigma_b = \frac{2EP_c}{A\sqrt{1 + (d_i/d_0)^2}} \frac{\partial^2 w}{\partial \xi^2} \tag{25}$$

For a preferred mode of buckling, w is given in the following form:

$$w(\xi, \tau) = g_p(\tau) \sin \eta_p \xi \tag{26}$$

Substituting the above equation into eqn (25) and using the modulus of the second derivative in eqn (25) gives

$$\sigma_b = \frac{\sigma_c g(\tau)}{\sqrt{1 + (d_i/d_0)^2}} \tag{17}$$

where $\eta_p = 1/\sqrt{2}$ from eqn (17) and $\sigma_c = P_c/A_s$ are used.

From eqns (22) and (27), the following equation is finally obtained:

$$\left[\frac{\sigma_c}{\sigma_y}\right]^{-1} = \frac{1}{0{\cdot}67}\left[1 + \frac{g_p(\tau)}{\sqrt{1 + (d_i/d_0)^2}}\right] \tag{28}$$

$g_p(\tau)$ in the above equation can be obtained numerically or from approximate solutions of eqns (12) and (13). In the calculation of $g_p(\tau)$, the non-dimensional initial imperfection a_p and damping coefficient ε can be found from eqns (21) and (10), respectively. Equation (28) is plotted in Fig. 2 for different damping coefficients and shows that the hydrodyamic damping force does not have a significant influence. Figure 3 is the result of buckling criteria for different initial deflections and denotes the relative importance of initial deflections. Therefore, for better accuracy of buckling criteria, more research into evaluating initial deflections is needed.

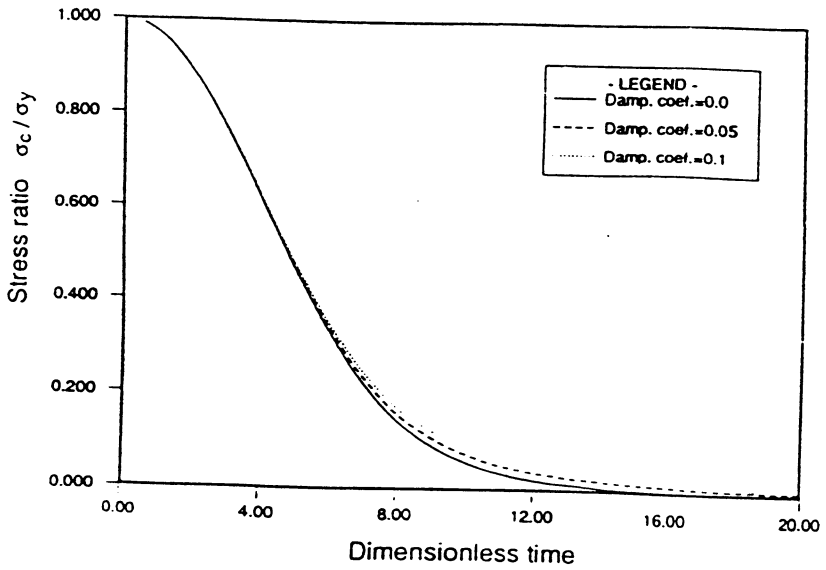

Fig. 2. Critical time and applied load to first yield for different damping coefficients, ε. $a_p = 0{\cdot}15$.

From these figures, the allowable applied compressive load ($P_c = \sigma_c A_s$) and duration time can be obtained for a slender cylinder subjected to compressive pulse axial load.

5 CASE STUDY AND CONCLUSIONS

The results of the above analysis are illustrated by a case study applied to relatively short tethers as used on the UK North Sea Conoco Hutton field TBP. Table 1 presents the nominal physical data used.

The case study is aimed at identifying an allowable envelope of axial compressive force against its duration. This would need to be used in conjunction with the extreme event statistics of tether tensions for the platform to determine a safe level of reduced mean tether tension. The resultant allowable envelope is presented in Fig. 4 as a plot of allowable compressive axial load on the vertical axis against duration in seconds on the horizontal axis. It can be seen that a significant axial load of 1 MN can be sustained for a maximum duration of 1 s and that loads of 0·24 MN can be acceptable for durations of over 5 s. Thus, for typical periods of high waves of from 14 to 20 s, the compressive load of 0·29 MN can be sustained for a significant proportion of half these wave periods.

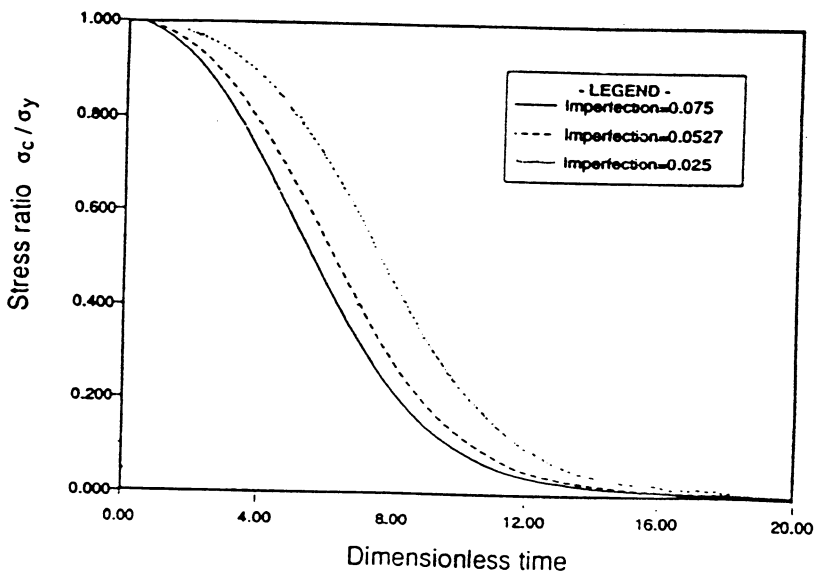

Fig. 3. Critical time and applied load to first yield for different imperfections. $\varepsilon = 0{\cdot}02$.

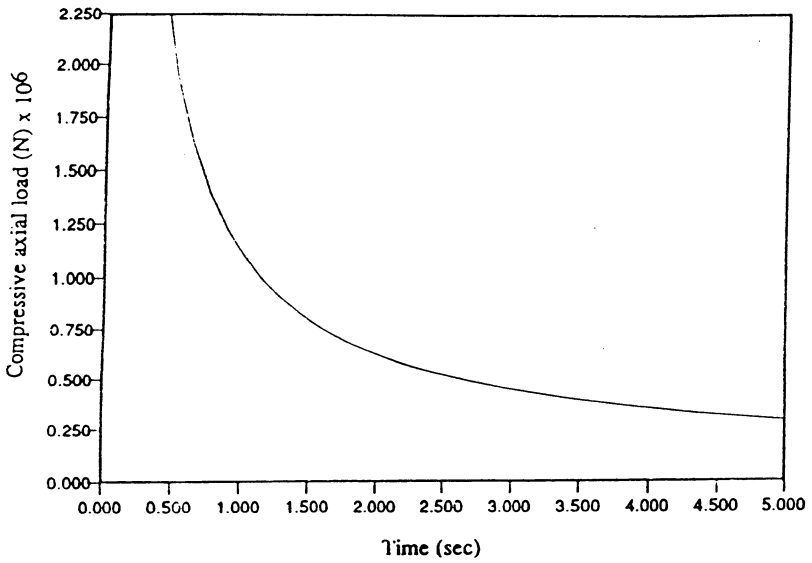

Fig. 4. Relationship between allowable compressive force and duration time for Hutton tether.

The results of this work can be compared with those of Brekke and Gardner[8] who carried out a numerical simulation for an example TBP to show that it can survive a momentary tether tension loss without causing large motions of the surface platform, large bending stresses in the tethers or significant tension amplification as the tethers undergo retensioning. Even though they did not provide the magnitude of the negative tension, the results from this work are in qualitative agreement with those presented by Brekke and Gardner.[8]

TABLE 1
Nominal Data for Hutton Tether

Length (m)	114·0
Top tension (N)	$8{\cdot}0 \times 10^{6}$
Flexural rigidity (N m^2)	$5{\cdot}29 \times 10^{}$
Outer diameter (m)	0·26
Inner diameter (m)	0·076
Dry mass (kg/m length)	472
Yield stress (MPa)	795
Drag coefficient	1·1

REFERENCES

1. Park, H. I., Dynamic stability and vibrations of slender marine structures at low tension. PhD thesis, University of London, UK, 1992.
2. Meier, J. H., On the dynamics of elastic buckling. *J. Aeronautical Sci.*, **12** (1945) 433–40.
3. Gerard, G. & Becker, H., Column behaviour under conditions of impact. *J. Aeronautical Sci.*, **19** (1952) 58–62.
4. Sevin, E., On the elastic bending of columns due to dynamic axial forces including effects of axial inertia. *J. Appl. Mechanics* (Transactions ASME), **27** (1960) 125–31.
5. Lindberg, H. E., Impact buckling of a thin bar. *J. Appl. Mechanics* (Transactions ASME), (1965) 315–22.
6. Holzer, S. M. & Eubanks, R. A., Stability of columns subjected to impulsive loading. *J. Engng Mechanics Div., ASCE*, **95** (EM4) (1969) 897–920.
7. Lindberg, H. E. & Florence, A. L., *Dynamic Pulse Buckling*. Martinus Nijhoff Publishers, 1987 p. 384.
8. Brekke, J. N. & Gardner, T. N., Analysis of brief tension loss in TLP tethers. *J. Offshore Mechanics Arctic Engng*, **110** (1988) 43–7.

KOREA MARITIME UNIVERSITY
1945
한국해양대학교